

DETERMINING THE SHAPE OF A PATTERN CLASS: EXTENSION TO \mathbb{R}^N

DEBA PRASAD MANDAL, C. A. MURTHY and SANKAR K. PAL

*Machine Intelligence Unit, Indian Statistical Institute,
203, Barrackpore Trunk Road, Calcutta—700-035, India*

(Received 12 April 1993; In final form 31 May 1996)

An important problem in pattern recognition is determining the shape of a pattern class from its sampled points. We have reported earlier a procedure in this regard which provides multivalued shape of a pattern class in \mathbb{R}^2 . In the present article, an extension of the procedure to higher dimensional space (N) has been suggested. The effectiveness of the extended version has been demonstrated on some artificially generated pattern classes (in \mathbb{R}^3). The convergence of the estimated shape to the original set has also been verified using two different metrics.

Index Terms: Set estimation; fuzzy sets; geometric complexity; windows; accuracy factor; goodness of fit

I. INTRODUCTION

Determining the pattern class and its shape from sampled points (or a set of training samples) in any dimension is an important problem in pattern recognition. There are various approaches described in the literature for determining the shape of a pattern class from sampled points in \mathbb{R}^2 [Edelsbrunner *et al.* 1983; Jarvis 1977; Akl *et al.* 1978; Fairfield 1979; Toussaint 1980; Preparata *et al.* 1985; Murthy 1988]. These methods are mostly heuristic in nature and/or they provide an exact boundary or shape of the pattern class. One of the inherent observations about these algorithms is that the boundary of the class is restricted by the sampled points. This needs not be true because the resulting boundary leaves certain regions not confined in it, although it should be. So, it is necessary to extend the boundaries to some extent to handle the possible uncovered portions by the sampled points. The extended portions should have the following two properties:

- (i) As the number of sampled points increases, the extended portions should decrease.

- (ii) The extended portions should have less possibility to be in the pattern class than the portions explicitly highlighted by the sampled points.

The second property leads to define a multivalued or fuzzy (with continuum grades of belongingness) boundary of a pattern class.

We have reported earlier [Mandal *et al.* 1992a] a procedure which deals with the problem of determining the pattern class and its multivalued shape/boundary from sampled points in \mathbb{R}^2 . The procedure initially deals with the decomposition of the sample set into some groups of nearly rectangular shape. Then it determines each of the subclasses corresponding to the groups separately, puts them together, and finds the multivalued shape of a pattern class. The effectiveness of the procedure was demonstrated on some artificially generated data sets (in \mathbb{R}^2) and also on a real life speech data set. The convergence of the estimated classes to the original ones was also verified using Hausdorff metric and another new metric *Sim*.

Some investigations on estimation of shapes for point sets in \mathbb{R}^3 were also carried out. The use of Delaunay triangulations to “sculpture” a single connected shape of a point set was suggested in [Boissonnat 1984]. The concept of α -shapes for the point sets in \mathbb{R}^3 has recently been proposed in [Edelsbrunner *et al.* 1992]. In the present paper, a procedure for finding shapes in higher dimensional spaces (\mathbb{R}^N , $N > 2$) is proposed which is an extension of our earlier work [Mandal *et al.* 1992a]. The procedure initially concerns with the decomposition of the sample set into some groups having nearly N-dimensional parallelepiped (henceforth parallelepiped) shape. Finally, combining the subclasses corresponding to the groups, the multivalued shape of a pattern class is determined. The effectiveness of the generalized methodology has been demonstrated on some artificially generated data sets in \mathbb{R}^3 . The convergence of the estimated classes to the original ones has also been verified.

In section II, some basic concepts and the block diagram of the multivalued shape determining procedure are provided. A brief description of the procedure for \mathbb{R}^2 is furnished in section III. The remaining sections of this article are concerned with the pattern classes in \mathbb{R}^N . Section IV deals with the procedure for decomposing a training sample set. Section V provides an approach to determine the multivalued boundary of a pattern class. Experimental results are provided in section VI. The convergence property is discussed in Section VII. Section VIII finds the conclusions and discussion. ♣

II. SOME BASIC CONCEPTS AND BLOCK DIAGRAM

Some of the basic concepts which are useful in developing the proposed method are initially stated here. The block diagram of the procedure is then provided.

A. Some Basic Concepts

a. Pattern class: In most of the real life problems, pattern classes are bounded. Thus the pattern classes considered here are all bounded. A formal definition of pattern class in \mathbb{R}^N is given below using topological and measure theoretic concepts.

DEFINITION 1: A set $\mathcal{A} \subseteq \mathbb{R}^N$ is said to be a pattern class [Murthy 1988] if

- (i) \mathcal{A} is path connected compact,
- (ii) $cl(Int(\mathcal{A})) = \mathcal{A}$, [cl means closure, Int means interior]
- (iii) $Int(\mathcal{A})$ is path connected and
- (iv) $\lambda(\delta\mathcal{A}) = 0$ where $\delta\mathcal{A} = \mathcal{A} \cap cl(\mathcal{A}^c)$ and λ is the Lebesgue measure on \mathbb{R}^N .

The relevance of the properties (i), (ii), (iii) and (iv) of Definition 1 is provided in [Murthy, 1988]. Let $\mathcal{B} = \{\mathcal{A} : \mathcal{A} \text{ satisfies Definition 1}\}$. \mathcal{B} is the collection of all classes in \mathbb{R}^N . Any $\mathcal{A} \in \mathcal{B}$ is referred to as the pattern class. •

b. Accuracy factor: It has been argued in the previous section that the regions not represented by the sampled points of a class should be included to some extent while determining its boundary. In other words, the regions covered by the sampled points should be extended to some degree for obtaining or estimating the shape of the class. For a given number of sampled points (t) in \mathbb{R}^N , an accuracy factor δ_t has been considered here to be [Grenander 1981] such that

$$\frac{1}{t^{1/N}} < \delta_t < \frac{1}{t^{1/(N+1)}} \quad (1)$$

so that as t increases, $\delta_t \rightarrow 0$ and $t\delta_t^N \rightarrow \infty$. Since δ_t decreases with the increase of t , the accuracy of the obtained boundary also increases with the increase of t . The selection of an accuracy factor is guided by the inequality (1) and its justification can be found in Mandal *et al.* [1992a] and Mandal [1992]. •

c. Coverage factors: Each individual sampled point represents a covered area of the pattern class in the feature space. As mentioned earlier, the extended portions should have less possibility to be in the pattern class than the portions explicitly highlighted by the sampled points. To decide on the amount of extension, a coverage factor is defined below corresponding to each feature axis.

Let $X_1, X_2, \dots, X_i, \dots, X_t$ be the training samples where $X_i = (x_{i1}, x_{i2}, \dots, x_{ij}, \dots, x_{iN})'$ and x_{ij} denotes the j th feature value of the i th sample. Let MAX_j and MIN_j denote the maximum and minimum feature values respectively in the sample set corresponding to the j th ($j = 1, 2, \dots, N$) feature i.e.,

$$MAX_j = \max_{i=1, 2, \dots, t} \{x_{ij}\} \quad \text{and} \quad MIN_j = \min_{i=1, 2, \dots, t} \{x_{ij}\}.$$

The *coverage factor* for the set of sampled points corresponding to the j th feature, denoted by ε_j ($j = 1, 2, \dots, N$), is defined as

$$\varepsilon_j = (\text{MAX}_j - \text{MIN}_j) \times \delta_i \quad (2)$$

where δ_i is the accuracy factor. When the number (t) of sampled points increases, the accuracy factor (δ_i) decreases, and correspondingly the values of the coverage factors (ε_j 's) also decrease, and the accuracy of the boundary increases. •

d. Hole in a pattern class: A path connected and compact set is referred to here as a pattern class. If it happens that within the range of the pattern class or set, some portions do not belong to the class, then the portions are referred to as the holes. The intuitive idea behind holes of a pattern class can be put mathematically by the following definition.

DEFINITION 2: A pattern class \mathcal{A} is said to have k holes if

$$\mathcal{A}^c = \mathcal{B} \cup C_1 \cup C_2 \cup \dots \cup C_k \quad \text{such that}$$

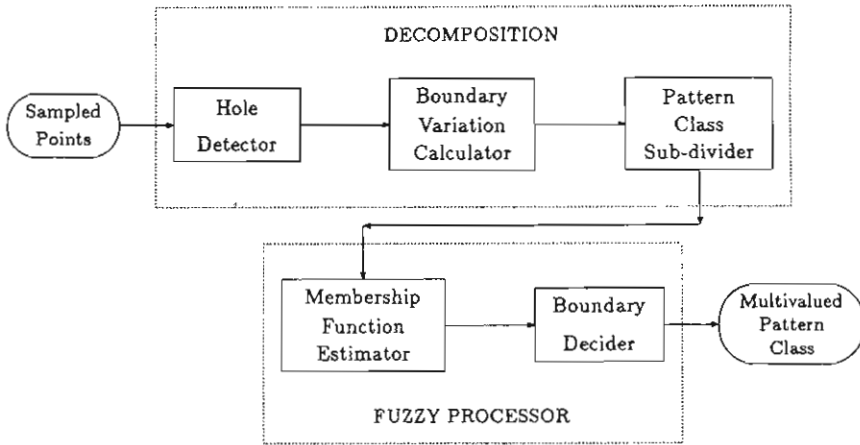
- (i) \mathcal{B} and C_i are path connected sets for $i = 1, 2, \dots, k$,
- (ii) \mathcal{B} is unbounded and C_1, C_2, \dots, C_k are bounded,
- (iii) $\mathcal{B} \cup C_{i_1} \cup C_{i_2} \cup \dots \cup C_{i_r}$ is a disconnected set for $1 \leq i_1 \leq i_2 \leq \dots \leq i_r \leq k$, where $1 \leq r \leq k$ and
- (iv) $C_{i_1} \cup C_{i_2} \cup \dots \cup C_{i_r}$ is a disconnected set $1 \leq i_1 < i_2 < \dots < i_r \leq k$, where $2 \leq r \leq k$.

Then C_1, C_2, \dots, C_k , in Definition 2, are said to be the holes of \mathcal{A} . The hole detection procedure for \mathbb{R}^2 can be found in Mandal *et al.* [1992a] and Mandal [1992], and it is described in section III.A for \mathbb{R}^N . ♣

B. Block Diagram

The block diagram of the multivalued shape determining procedure is shown in Fig. 1 [Mandal *et al.* 1992a]. It consists of two parts, namely the *decomposition* and the *fuzzy processor*. The decomposition section deals with the decomposition of the sample set into some groups of nearly parallelepiped shape. The fuzzy processor determines each of the subclasses corresponding to the sample groups separately and all these subclasses are then combined to compute the multivalued shape of the pattern class.

The decomposition section consists of three blocks as shown in Fig. 1. The *hole detector* block decomposes the training sample set with holes into groups to find

FIGURE 1 Block diagram [Mandal *et al.* 1992a].

the hole information. The *boundary variation calculator* block finds the values of the boundary variation factors corresponding to all possible boundary directions. These boundary variation values are analyzed in the *pattern class sub-divider* block to decompose (if necessary) the sample set into groups.

Concepts of fuzzy sets [Zadeh 1965; Zadeh 1973; Pal *et al.* 1986; Bezdek 1981; Bezdek *et al.* 1992; Kandel 1982; Yager *et al.* 1992] have been used in the fuzzy processor to extend the boundary of the sample set and also to relate every point in the whole feature space to its possibility to be in the pattern class. The *membership function estimator* block decides about the compatibility/membership functions to represent each of the subclasses corresponding to the sample groups. The *boundary decider* block determines each of the subclasses separately, puts them together and finds the multivalued shape of a pattern class. ♣

Before explaining the operations of different blocks for a pattern class in \mathbb{R}^N , a short description of the procedure for \mathbb{R}^2 [Mandal *et al.* 1992a] is provided in the next section. ▲

III. DETERMINING MULTIVALUED SHAPE IN \mathbb{R}^2

The decomposition section takes the set of sampled points of a pattern class as an input and decomposes the training sample set (in \mathbb{R}^2) into some groups of nearly rectangular shape. To obtain this decomposition, a procedure based on some overlapping windows was adopted [Mandal *et al.* 1992a]. Before describing the

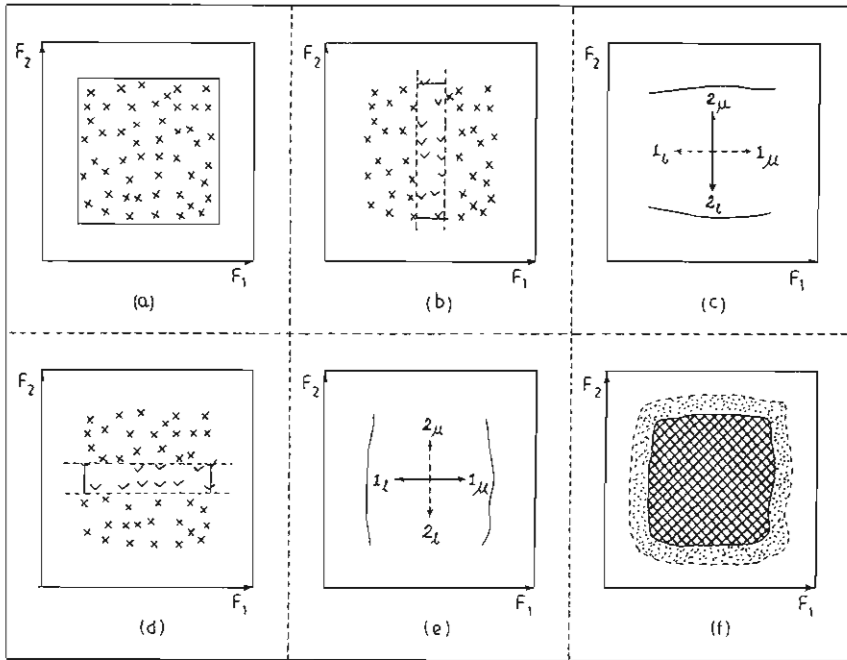
operations of various blocks of decomposition, the approach to generate the windows and the concept of (multivalued) boundary are furnished below.

Generation of windows: The two features under consideration are referred to as the first (F_1) and second (F_2) feature axes respectively. One of the axes is considered here as the base axis and the other axis is considered as the height axis. Consequently the coverage factors corresponding to the base and height features are referred to as the *base coverage factor* (ε_b) and *height threshold factor* (ε_h) respectively.

The sampled points are first of all arranged in ascending order according to the base feature values. The first window starts with the first sample of the ordered sample set and it includes all those samples one after another in ascending order until its base coverage length exceeds ε_b . Assume that the generated first window ends with the k th sample of the ordered sample set. That is, the first window is constructed in such a way that the range of the base features exceeds ε_b for the first time by including the k th ordered sample. The construction of the second window with the same base feature is such that it will end with the $(k + 1)$ th sample. To find the starting sample point of this window, it proceeds backward from $(k + 1)$ th sample until the base coverage length exceeds ε_b for the first time. Similarly other windows are constructed by including one new sample at the end and excluding some samples from the beginning of the previous window such that the base coverage length would at least be ε_b . The last window ends with the last ordered sample i.e., the sample with the highest base value. Thus, some overlapping windows of the sample points are generated utilizing the sample base values and the base coverage factor (ε_b).

The maximum and the minimum height values are found for each of the windows and these are taken to be the upper (u) and lower (l) boundary values respectively of that window. The combination of the upper boundary values highlights the upper boundary of the training sample set for that feature and the combination of the lower boundary values provides the lower boundary of the training sample set for that feature. Putting together the upper boundaries and lower boundaries of all the features provide the complete boundary of the set.

The way in which the boundary of a training sample set is obtained using the aforementioned procedure of generating windows, is now explained considering a typical pattern class [Fig. 2(a)]. A hypothetical training sample set is shown in Fig. 2(a), where the locations of samples in the feature space are shown by cross (\times) marks. Initially, F_1 is considered as the base, and a few overlapping windows are generated. In such windows, F_2 is considered as the height feature. A typical window is shown by dotted lines in Fig. 2(b) where the samples in the window are shown by tick (\surd) marks. The boundary values corresponding to the lower(l) and upper(u) directions (referred to as 2_l and 2_u respectively) are also marked for the

FIGURE 2 Illustrating the concept of boundary in \mathbb{R}^2 .

window. Based on these boundary values, the rough boundaries in the coded directions 2_l and 2_u are drawn in Fig. 2(c). To find the boundaries in the lower and upper directions of F_1 (i.e., directions 1_l and 1_u), some overlapping windows are first of all generated considering F_2 as the base feature. A typical window with its sample points and boundary values is shown in Fig. 2(d). Fig. 2(e) shows the rough boundaries in the coded directions 1_l and 1_u .

Combining the boundaries in figures 2(c) and 2(e), the complete boundary of a pattern class is obtained [Fig. 2(f)]. To incorporate the possible uncovered portions of the pattern class by the training set [Fig. 2(a)], these boundaries are extended to some extent (depending on the coverage factors). To visualize the said extension, the extended boundary of the pattern class is conceptually drawn in Fig. 2(f). The extended portion should have lower possibility to be in the class than the portions explicitly highlighted by the sample points. The extended regions decrease with the increase of the sample size (t). •

The hole detector block decomposes the training sample set into groups to find the hole information. When the subclasses corresponding to the sample groups are combined later, the holes are excluded from the final shape of the pattern class.

The boundary variation calculator block detects the geometric structure of the pattern class from a set of sampled points. The boundaries in four perpendicular directions [Fig. 2(b)] are considered to find the boundary variation factors.

The pattern class sub-divider block analyzes the *boundary variation factors* to determine whether the training sample set is to be decomposed or not. Based on the direction for which the variation factor is maximum, the sample set is decomposed into groups of nearly rectangular shape.

The fuzzy processor section initially finds the subclasses corresponding to the sample groups. Finally it combines them to get the estimated multivalued shape of the pattern class. The concept of membership functions in the light of fuzzy set theory was brought in here to represent each of the subclasses corresponding to the groups separately. Membership functions have also been used to relate every point (referred to as Feature Space Cell or FSC) in the entire feature space to its possibility to be in the pattern class. The membership function estimator block finds the appropriate membership functions to represent each of the subclasses corresponding to the sample groups. The boundary decider block determines each of the subclasses separately, puts them together and obtains the multivalued shape of the pattern class.

The effectiveness of the procedure for \mathbb{R}^2 was demonstrated [Mandal *et al.* 1992a] on some artificially generated data sets as well as on a real life speech data set. Fig. 3(a) shows a pattern class as considered in [Mandal *et al.* 1992a]. A training sample set of size 50 is shown in Fig. 3(a). Based on this sample set, the estimated multivalued set of the class is shown in Fig. 3(b) with 0.15 as the accuracy factor (δ_r). ♣

The extension of the procedure to the pattern classes in \mathbb{R}^N ($N > 2$) is furnished in the following sections. As in the case of \mathbb{R}^2 , we first decompose (based on a window approach) the training sample set into some groups of nearly N -dimensional parallelepiped (henceforth parallelepiped) shapes and these are then combined to find the final shape of the pattern class (in \mathbb{R}^N). ♠

IV. DECOMPOSITION

A pattern class in \mathbb{R}^N is represented here by a set of sampled points. The decomposition section detects the geometric structure of the pattern class from the sample set. The N features under consideration are referred to as the first (F_1), second (F_2), . . . , N th (F_N) axes respectively. Initially the window generation procedure from a sample set in \mathbb{R}^N is described. The generalized methodology for finding the shape is then elaborated using the window generation procedure.

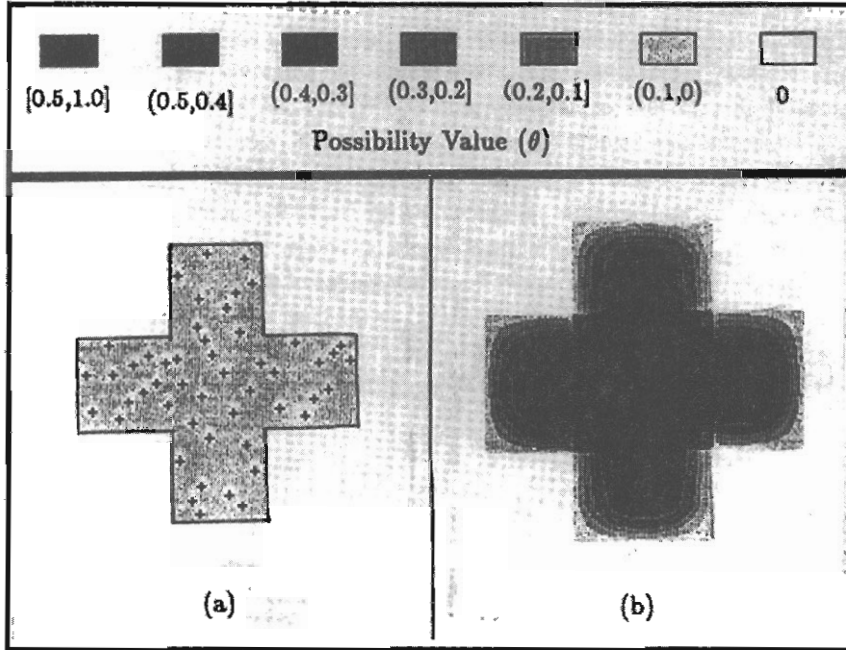


FIGURE 3 (a) A typical pattern class with a set of sampled points; (b) Estimated (multivalued) shape of the class.

Generation of windows: Similar to the case of \mathbb{R}^2 , a window based approach is adopted here to find the boundary variations of a sample set in \mathbb{R}^N . Initially, one of the feature axes is considered as the base feature and the corresponding coverage factor is referred to as the base coverage factor (ε_b). The training samples are first of all arranged in ascending order according to the base feature values. Then, depending on the base feature values and the base coverage factor ε_b , the same procedure, as stated for \mathbb{R}^2 , is followed here to generate windows. These windows are such that base coverage length of each window would atleast be ε_b .

Here for a particular window, the base feature values of the samples are assumed to be the same and the rest $(N-1)$ features for the samples may take any value. So the generated windows are visualized here to belong to \mathbb{R}^{N-1} ; although the original sample set belongs to \mathbb{R}^N . In this sense, the proposed method of generating windows always results in reducing the dimension of the sample set by one. In this context, note that, the initial training sample set may itself be considered to belong to an N -dimensional window.

Based on the aforesaid concepts, the multivalued shape determining procedure is extended to \mathbb{R}^N . The approach has been applied on a sample set in \mathbb{R}^N in the

following way. To start with, the feature F_{i_1} is considered as the base feature and correspondingly a few windows in \mathbb{R}^{N-1} are formed. For each of these windows, another axis F_{i_2} is considered as the base feature and windows in \mathbb{R}^{N-2} are formed. Repeating this process sequentially with $F_{i_3}, F_{i_4}, \dots, F_{i_{N-1}}$ as the base features axes, some one-dimensional $(1-D)$ windows are generated eventually. The values of the left out feature F_{i_N} are considered here as the height values. The maximum and the minimum height sample values are found for each window and these are taken to be the upper and the lower *boundary values* respectively for that window. The combination of the upper boundary values of all $1-D$ windows, generated by sequentially taking $F_{i_1}, F_{i_2}, \dots, F_{i_{N-1}}$ as the base axes, highlights the upper boundary of the training sample set in the F_{i_N} feature direction. Similarly, the combination of the lower boundary values provides the lower boundary of the sample set across F_{i_N} axis.

A. Hole Detector

The operation of this block is same as that described in Mandal *et al.* [1992a]. The procedure sequentially considers F_1, F_2, \dots, F_{N-1} as the base features (and correspondingly $\varepsilon_1, \varepsilon_2, \dots, \varepsilon_{N-1}$ as the base coverage factors) to generate few $1-D$ windows with F_N as the height feature. Here the coverage factor ε_N across the axis F_N is referred to as the height threshold factor. The samples in each window are then arranged in ascending order according to the height (F_N) sample values. If the difference of height values of any two consecutive samples within a window exceeds ε_N , then a hole is assumed to be present between the said sample pair. Let h' and h'' be the height feature values of two such sample points. To detect the hole, the sample set is decomposed into two groups according to whether the height values (i.e., F_N values) are less than $(h' + h'')/2$ or not.

The aforesaid routine is repeated until every sample group is found to be not containing any hole. When the subclasses corresponding to the sample groups are combined later in the boundary decider block, the holes are excluded from the final shape of the pattern class. •

B. Boundary Variation Calculator

To find the boundary variations of the sample set in \mathbb{R}^N , $2N$ perpendicular directions (coded as $1_l, 1_u, 2_l, 2_u, \dots, N_l, N_u$) corresponding to the lower and upper boundary directions along the N feature axes are considered. The N features are denoted here by $F_{i_1}, F_{i_2}, \dots, F_{i_N}$ such that $i_k \in \{1, 2, \dots, N\}$ for $k = 1, 2, \dots, N$ and $i_k \neq i_{k'}$ for $k \neq k'$. The procedure to find the boundary variation values is described below for a training sample set in \mathbb{R}^N . Though the notation used here

may seem to be little cumbersome, it may be noted that the procedure is the natural extension of the 2-D case (described in Mandal *et al.* [1992a]).

Initially assuming the feature F_{i_1} as the base (and correspondingly ε_{i_1} as the base coverage factor), some windows are generated from the total training set. Let the number of windows generated be denoted by q_{i_1} . As mentioned earlier, in each of these q_{i_1} windows, the F_{i_1} feature values of the samples are considered to be the same and so the samples are visualized to belong in \mathbb{R}^{N-1} with $F_{i_2}, F_{i_3}, \dots, F_{i_N}$ as the feature axes. Let a particular window, say j_1 th one, be denoted by $W_{i_1}^{j_1}$ where $j_1 = 1, 2, \dots, q_{i_1}$. Now assuming the feature F_{i_2} as the base (and correspondingly ε_{i_2} as the base coverage factor), the sample set of the window $W_{i_1}^{j_1} (\in \mathbb{R}^{N-1})$ results in $q_{i_1(i_2)}^{j_1(j_2)}$ windows in $(N-2)$ dimensional space with $F_{i_3}, F_{i_4}, \dots, F_{i_N}$ as the feature axes. Similarly, considering sequentially the features $F_{i_3}, F_{i_4}, \dots, F_{i_{N-2}}$ as the bases (and correspondingly $\varepsilon_{i_3}, \varepsilon_{i_4}, \dots, \varepsilon_{i_{N-2}}$ as the respective base coverage factors), some 2-D windows will be generated and the number of such windows is denoted by $q_{i_1(i_2 \dots (i_{N-3}(i_{N-2})))}^{j_1(j_2 \dots (j_{N-3}))}$ (where $j_k = 1, 2, \dots, q_{i_1(i_2 \dots (i_{k-1}(i_k)))}$, for $k = 1, 2, \dots, N-3$). These windows are visualized here to belong to \mathbb{R}^2 with $F_{i_{N-1}}$ and F_{i_N} as the axes. Thus the original sample set (belonging to \mathbb{R}^N), after the aforementioned operations, gives rise to a collection of 2-D windows.

The feature $F_{i_{N-1}}$ is now assumed to be the base (and correspondingly $\varepsilon_{i_{N-1}}$ is assumed as the base coverage factor) so that the samples of the j_{N-2} th window $W_{i_1(i_2 \dots (i_{N-2}(i_{N-1})))}^{j_1(j_2 \dots (j_{N-2}))}$ results in $q_{i_1(i_2 \dots (i_{N-2}(i_{N-1})))}^{j_1(j_2 \dots (j_{N-2}))}$ 1-D windows with F_{i_N} as the feature axis. For the samples belonging to these 1-D windows, the values of F_{i_N} are now considered as the height values. The maximum and the minimum height sample values are found in each of the 1-D windows and these are taken as the upper and the lower boundary values respectively for the respective windows.

Let $H_{i_1(i_2 \dots (i_{N-2} \dots))}^{j_1(j_2 \dots (j_{N-2}))}$ denote the boundary value of the k th ($k = 1, 2, \dots, q_{i_1(i_2 \dots (i_{N-2}(i_{N-1})))}^{j_1(j_2 \dots (j_{N-2}))}$) 1-D window (generated by taking $F_{i_{N-1}}$ as the base) for the feature F_{i_N} in the direction d ($d \in \{l, u\}$ where l and u stand for lower and upper boundary directions respectively). For each of the $q_{i_1(i_2 \dots (i_{N-3}(i_{N-2})))}^{j_1(j_2 \dots (j_{N-3}))}$ 2-D windows, the upper and the lower boundary variation factors, denoted by $V_{i_1(i_2 \dots (i_{N-1} \dots))}^{j_1(j_2 \dots (j_{N-2}))}$, are defined based on their respective 1-D windows as follows

$$V_{i_1(i_2 \dots (i_{N-1} \dots))}^{j_1(j_2 \dots (j_{N-2}))} = \left[\sum_{k=2}^{q_{i_1(i_2 \dots (i_{N-2}(i_{N-1})))}^{j_1(j_2 \dots (j_{N-2}))}} \left(H_{i_1(i_2 \dots (i_{N-2} \dots))}^{j_1(j_2 \dots (j_{N-2}))} : d : k} - H_{i_1(i_2 \dots (i_{N-2} \dots))}^{j_1(j_2 \dots (j_{N-2}))} : d : k-1} \right)^2 \right] / \varepsilon_{i_N}^2 \quad (3)$$

$$j_{N-2} = 1, 2, \dots, q_{i_1(i_2 \dots (i_{N-3}(i_{N-2})))}^{j_1(j_2 \dots (j_{N-3}))} \quad \text{and} \quad d \in \{l, u\}$$

where ε_{i_N} is the coverage factor for the feature F_{i_N} . Here the division factor $\varepsilon_{i_N}^2$ is used to make the variation factor unitless.

Now, let MAX_H and MIN_H be the maximum and minimum of the boundary values respectively in a particular direction d and corresponding to a particular two dimensional window $W_{i_1(i_2(\dots(i_{N-2})\dots))}^{j_1(j_2(\dots(j_{N-2})\dots))}$. If the difference of MAX_H and MIN_H does not exceed ε_{i_N} (i.e., if $(MAX_H - MIN_H) \leq \varepsilon_{i_N}$), then the *boundary variation* for F_N in the direction d corresponding to the said 2-D window is considered to be insignificant. In such a case, the *variation factor* is assumed to be zero i.e., make $V_{i_1(i_2(\dots(i_{N-1})\dots))}^{i_N \ d: j_{N-2}} = 0$. Otherwise the sample set is considered to be decomposable in the direction d for F_N .

Note that the order in which the features have been considered for the previous generation of windows in \mathbb{R}^2 is i_1, i_2, \dots, i_{N-2} . It may be observed that for every such sequence, a set of 2-D windows is generated. Thus, all possible such sequences of features are considered and correspondingly boundary variation factors for the lower and upper boundaries across the left over two features are calculated for each of the 2-D windows.

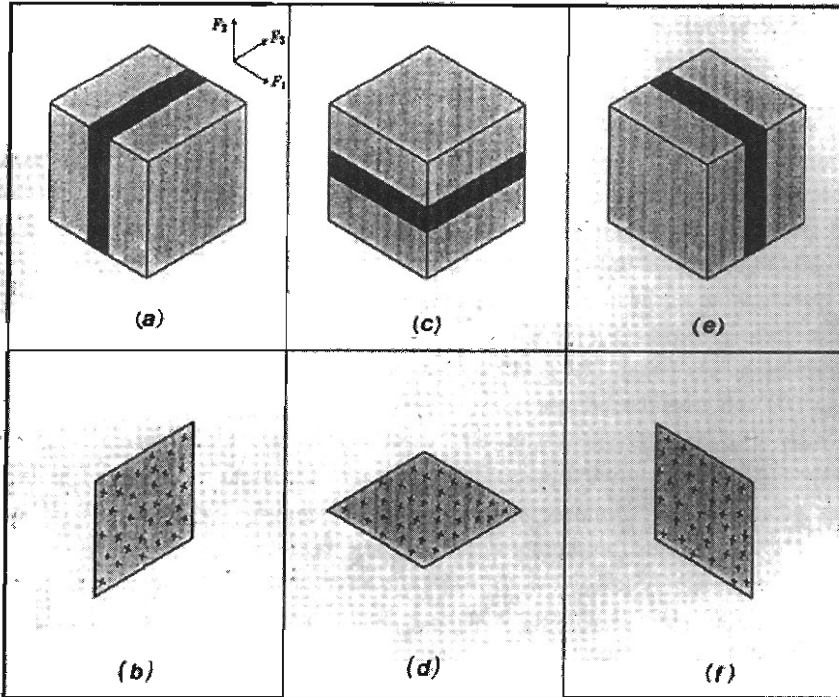
Pattern classes in \mathbb{R}^3 : As the notations used to describe the generalized approach seem to be little cumbersome, the procedure is now explained for the pattern class in \mathbb{R}^3 . For a better understanding, a cubic shaped pattern class, as shown in Fig. 4(a) is considered. Initially, F_1 is assumed to be the base feature to generate q_1 2-D windows. A typical (say, j_1 th) window $W_1^{j_1}$ ($j_1 = 1, 2, \dots, q_1$) is distinctly marked in Fig. 4(a). The 2-D view of this window with some typical training samples is shown in Fig. 4(b) where the F_1 feature is taken to be same (as the mid value of the ranges of F_1 in the window). Then considering F_2 as the base, the sample set of the window $W_1^{j_1}$ results in $q_{1(2)}^{j_1}$ windows in F_3 feature space. Now find the boundary values of each of $q_{1(2)}^{j_1}$ 1-D windows, which are denoted by $H_{1(2)}^{3: d: k}$ ($k = 1, 2, \dots, q_{1(2)}^{j_1}$ and $d \in \{l, u\}$). Based on these boundary values, the boundary variation factors of F_3 in direction d corresponding to their 2-D windows are calculated using Eq. (3) as follows

$$V_{1(2)}^{3: d: j_1} = \left[\sum_{k=1}^{q_{1(2)}^{j_1}} (H_{1(2)}^{3: d: k} - H_{1(2)}^{3: d: k-1})^2 \right] / \varepsilon_3^2$$

$$j_1 = 1, 2, \dots, q_1 \quad \text{and} \quad d \in \{l, u\}.$$

Similarly, by taking F_3 as the base feature, every sample window $W_1^{j_1}$ (generated by assuming F_1 as the base on the original sample set), gives rise to $q_{1(3)}^{j_1}$ 1-D windows in F_2 feature space. Finally the boundary variation factors of F_2 in the lower and upper boundary directions corresponding to their 2-D windows are obtained. So for all the above q_1 2-D windows, the boundary variation factors $V_{1(2)}^{3: l: j_1}, V_{1(2)}^{3: u: j_1}, V_{1(3)}^{2: l: j_1}, V_{1(3)}^{2: u: j_1}$ ($j_1 = 1, 2, \dots, q_1$) are calculated.

If F_2 is initially taken to be the base, the original sample set results in q_2 2-D windows with F_1 and F_3 as the feature axes. A typical of such windows is marked

FIGURE 4 Concept of windows for a pattern class in \mathbb{R}^3 .

in Fig. 4(c). The 2-D view of the marked window is provided in Fig. 4(d). Corresponding to each of the q_2 2-D windows, the boundary variation factors $V_{2(1)}^{3:l;j_2}, V_{2(1)}^{3:u;j_2}, V_{2(3)}^{1:l;j_2}, V_{2(3)}^{1:u;j_2}$ ($j_2 = 1, 2, \dots, q_2$) are obtained.

If F_3 is first considered to be the base, the initial sample set results in q_3 2-D windows with F_1 and F_2 as the feature axes. A typical windows is marked in Fig. 4(e) and its 2-D view is provided in Fig. 4(f). Corresponding to each of the q_3 2-D windows, the boundary variation factors $V_{3(1)}^{2:l;j_3}, V_{3(1)}^{2:u;j_3}, V_{3(2)}^{1:l;j_3}, V_{3(2)}^{1:u;j_3}$ ($j_3 = 1, 2, \dots, q_3$) are determined.

Thus, there are in total $4(q_1 + q_2 + q_3)$ boundary variation factors corresponding to a sample set in \mathbb{R}^3 . All these variation factors are analyzed in the next block i.e., pattern class sub-divider block. •

C. Pattern Class Sub-divider

This block analyzes the boundary variation factors to determine whether the training sample set is to be decomposed or not. To decide this, it finds the maximum of all the variation factors. If this value is zero, then the sample set is assumed to

be nearly parallelepiped in shape and it is not further decomposable. Otherwise it is assumed that the sample set is not nearly parallelepiped in shape and it is to be decomposed into few groups. Corresponding to the 2-*D* window and the direction of the maximum variation factor, the 1-*D* windows with their base and boundary values, and the coverage factor corresponding to the height feature (referred to as height threshold factor ε_h) are marked. Based on these values, the decomposition is made. The samples in the particular 2-*D* window are then arranged in ascending order according to the base values.

For making a cluster of 1-*D* windows, the maximum boundary value is found. The starting window for the cluster is taken as the 1-*D* window having the maximum boundary value. The position of the starting window is noted. The following 1-*D* windows from the starting windows are assigned one after another in the cluster until the differences between the boundary values of the current 1-*D* window and the starting window exceeds the height threshold factor (ε_h). Similarly the preceding 1-*D* windows are also put in the window cluster. The maximum (say, MAX_b) and the minimum (say, MIN_b) base values of the samples in the window cluster are found. Now from all the samples in the considered sample set/group, the samples with the base lying between MIN_b and MAX_b are assigned to the first sample group.

The aforesaid routine is repeated on the remaining 1-*D* windows until all the marked 1-*D* windows are exhausted. This leads to the formation of window clusters. Every window cluster results in a group of sample points. Thus, the given training sample set is decomposed into a few groups of sample points.

The decomposition procedure is applied on each of the sample groups repeatedly until all the groups are found to be nearly parallelepiped in shape. ♣

V. FUZZY PROCESSOR

A training sample set is decomposed in the previous section into few groups of nearly parallelepiped shape. Here the subclasses corresponding to these groups are determined separately and finally these are combined to obtain the multi-valued shape of the pattern class.

A. Membership Function Estimator

For any feature point, the possibility of being a member of a class is maximum if it lies in the centre of the class. As its distances from the the centre increases, the membership value decreases and ultimately goes to zero. Any function having

this property may be considered as the representative membership function for the (sub) pattern class corresponding to a sample group. As the π function is well established to dictate this property [Pal *et al.* 1986; Zadeh 1965; Zadeh 1973], it is considered here as the representative membership function.

Thus, the subclasses corresponding to the sample groups are characterized by different π functions across different axes of the form $\pi(x; \alpha_{k_j}, \beta_{l_{k_j}}, \beta_{u_{k_j}}, \gamma_{l_{k_j}}, \gamma_{u_{k_j}})$ where k indicates the group number ($k = 1, 2, \dots, \eta$, η denotes the number of groups); j indicates the axis number ($j = 1, 2, \dots, N$); α_{k_j} is the peak value where the membership value is 1.0; $\beta_{l_{k_j}}$ and $\beta_{u_{k_j}}$ are the lower and upper most ambiguous points where the membership values are 0.5, and $\gamma_{l_{k_j}}$ and $\gamma_{u_{k_j}}$ are the lower and upper end points beyond which the membership values are zero. The structure and the functional form of such a π function can be found in Mandal *et al.* [1992a] and Mandal [1992].

Determination of membership functions: To determine the membership functions (which are taken as π functions), the parameters of them corresponding to various sample groups are to be evaluated. Here each of the sample groups is considered separately. Let MAX_{k_j} and MIN_{k_j} be the maximum and minimum of the training sample set respectively corresponding to j th ($j = 1, 2, \dots, N$) feature and k th ($k = 1, 2, \dots, \eta$) sample group. Then the parameters of the π function corresponding to j th feature and k th subclass (i.e., k th sample group) are assigned as follows:

$$\begin{aligned} \alpha_{k_j} &= \frac{MAX_{k_j} + MIN_{k_j}}{2} ; \\ \beta_{l_{k_j}} &= MIN_{k_j} ; \beta_{u_{k_j}} = MAX_{k_j} ; \\ \gamma_{l_{k_j}} &= MIN_{k_j} - \varepsilon_j ; \gamma_{u_{k_j}} = MAX_{k_j} + \varepsilon_j ; \\ j &= 1, 2, \dots, N ; k = 1, 2, \dots, \eta ; \end{aligned} \quad (4)$$

where ε_j is the coverage factor for the j th feature [Eq. (2)].

B. Boundary Decider

In the previous subsection, membership functions corresponding to all the sample groups along each feature axis are determined. Using these functions, each of the subclasses corresponding to the sample groups is estimated and those are finally combined to obtain the estimated (multivalued) shape of the pattern class. All the points in the feature space are labeled with their degree of possibilities to be in the class. To show the shape of a pattern class in the feature space, the entire feature range is divided into small units of parallelepiped shape and these small units are referred to as the Feature Space Cell or FSC. The size of all the FSCs are same and these are made as small as possible such that each FSC can be

distinguished in the feature space. Thus, all these FSCs are labeled in terms of their possibility values to be in the pattern class. The FSCs with zero possibility value are considered to be outside the class. The method of obtaining these possibility values is described below.

Procedure: Let $(x_1, x_2, \dots, x_N)'$ be a typical feature value of such a FSC. The membership value (μ_{k_j}) of the FSC corresponding to k th ($k = 1, 2, \dots, \eta$) subclass (i.e., k th sample group) and j th ($j = 1, 2, \dots, N$) feature is calculated from the corresponding π function i.e.,

$$\mu_{k_j} = \pi(x_j; \alpha_{k_j}, \beta_{l_{k_j}}, \beta_{u_{k_j}}, \gamma_{l_{k_j}}, \gamma_{u_{k_j}}) \quad (5)$$

The combined membership (μ_k) of the FSC corresponding to k th ($k = 1, 2, \dots, \eta$) subclass is defined as the geometric mean of μ_{k_j} 's i.e.,

$$\mu_k = (\mu_{k_1} \times \mu_{k_2} \times \dots \times \mu_{k_N})^{1/N} \quad (6)$$

Now, the possibility, say θ , of the FSC to be in the estimated pattern class is defined as the maximum of the membership values of the subclasses. That is,

$$\theta = \max_{k=1, 2, \dots, \eta} \{\mu_k\} \quad (7)$$

Let τ be the number of subclasses for which the combined membership values $(\mu_k$'s) of the said FSC are positive. To incorporate the effect of the neighboring subclasses with positive membership values in the estimated pattern class, the value of θ is increased to $\theta^{1/\tau}$ for $\tau > 1$. That is, when the possibility values of the FSC $(\mu_k$'s) are positive for two or more subclasses, then it indicates that the said FSC has the possibility to lie in those subclasses, which in turn increases the possibility of the FSC to be in the finally obtained pattern class. •

The aforesaid method finds the possibility value (θ) of a FSC to be in the pattern class. Note that $0 \leq \theta \leq 1$. If the value of θ is zero, then the FSC is considered to lie outside the pattern class. Otherwise the FSC belongs to the pattern class with the possibility θ .

To obtain the complete shape of the pattern class, the aforesaid routine is repeated for every FSC in the feature domain. Thus, all the FSCs are labeled with their possibility values to be in the pattern class, and as a result, the multivalued shape of the pattern class is obtained. ♣

In the next section, the implementation and the usefulness of the generalized procedure are discussed. ♣

VI. IMPLEMENTATION AND RESULTS

The effectiveness of the proposed generalized shape determining procedure is demonstrated here with three artificially generated pattern classes in \mathbb{R}^3 . The classes are shown in figures 5(a), 6(a) and 7(a). For all 3-D classes, the isometric views are provided. Note that Fig. 7(a) shows only the lower bisecting (with respect to F_2 feature) portion of a pattern class which has the same external view with the class in Fig. 5(a). Actually this class is having a hole and externally the hole can not be shown. For demonstrating the hole detecting capabilities of the proposed generalized method, only the lower bisecting portion of a pattern class is displayed in Fig. 7(a).

Training samples of size 150 are chosen randomly from each of the three classes and correspondingly the accuracy factor (δ_i) is assumed to be 0.20. Note that the extracted classes are multivalued. Hence, in order to demonstrate the concept of the multivalued shapes, three levels of estimated classes based on the possibility values (θ), namely $\theta \geq 0.5$, $\theta \geq 0.25$, $\theta > 0$ are only shown. Figures 5(b), 5(c) and 5(d) show the estimated shapes with $\theta \geq 0.5$, $\theta \geq 0.25$, $\theta > 0$ respectively corresponding to the pattern class in Fig. 5(a). Figures 6(b), 6(c) and 6(d) show the estimated shapes with $\theta \geq 0.5$, $\theta \geq 0.25$, $\theta > 0$ respectively corresponding to the pattern class in Fig. 6(a). Figures 7(b), 7(c) and 7(d) show the lower bisected portion of the estimated shapes with $\theta \geq 0.5$, $\theta \geq 0.25$, $\theta > 0$ respectively corresponding to the lower bisected portion as shown in Fig. 7(a) of a pattern class.

To give a 3-D feeling of the training sets, the patterns of the class in Fig. 5(a) are shown in Fig. 8. Dotted lines corresponding to all the sample points are drawn from the $F_1 \times F_3$ feature plane (with F_2 as the minimum value in the pattern class). The actual locations of the sample points are distinctly marked. Based on this sample set, the output as shown in figures 5(b), 5(c) and 5(d) with $\theta \geq 0.5$, $\theta \geq 0.25$, $\theta > 0$ respectively are obtained. ♣

VII. CONVERGENCE WITH SAMPLE SIZE

Convergence of the estimated pattern class to the original pattern class in \mathbb{R}^2 was dealt with in Mandal *et al.* [1992a]. The same property can be shown for any dimension $N > 2$. For the sake of understanding and convenience in representation, we have demonstrated here for $N = 3$.

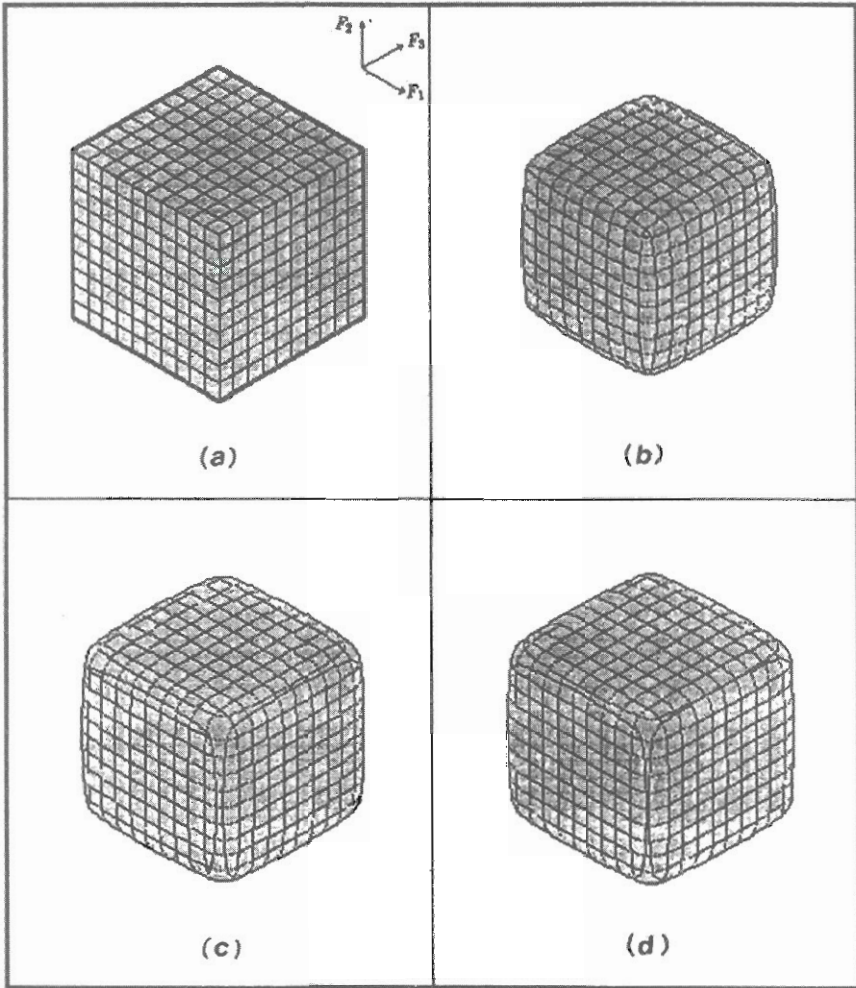


FIGURE 5 (a) A pattern class; (b)–(d) corresponding estimated versions with $\theta \geq 0.5$, $\theta \geq 0.25$, $\theta > 0$ respectively.

A. Experimental Verification

The convergence property has been demonstrated for a pattern class of spherical shape [Fig. 9] with radius 2 and centre at (3, 3, 3). Four different sets of data are chosen randomly from it with sizes 150, 300, 500 and 1200 respectively and the values of δ_i are considered as 0.20, 0.16, 0.13 and 0.10 respectively. Here also three levels of extracted classes are shown corresponding to $\theta \geq 0.5$, $\theta \geq 0.25$, $\theta > 0$. Figures 10(a)–(d) show the estimated classes with $\theta \geq 0.5$ based on the

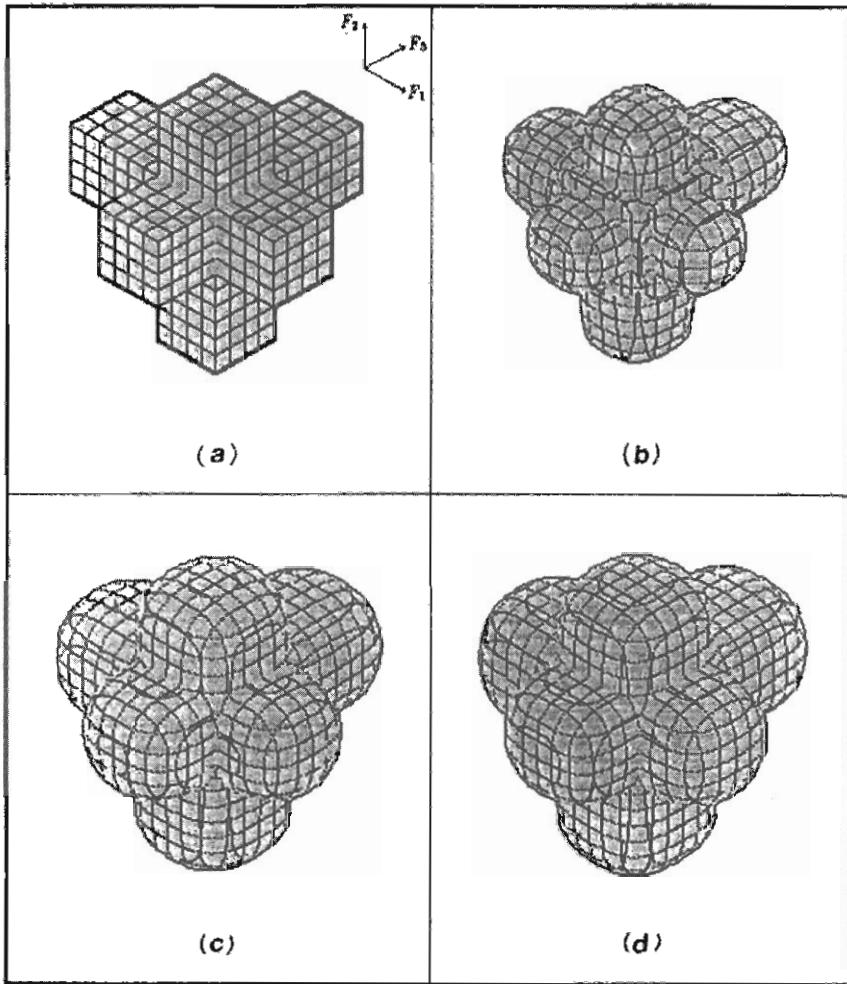


FIGURE 6 (a) A pattern class; (b)–(d) corresponding estimated versions with $\theta \geq 0.5$, $\theta \geq 0.25$, $\theta > 0$ respectively.

selected sample sets of sizes 150, 300, 500 and 1200 respectively corresponding to the pattern class in Fig. 9. Figures 11(a)–(d) show the estimated classes with $\theta \geq 0.25$ based on 150, 300, 500 and 1200 training samples respectively. Figures 12(a)–(d) show the estimated classes with $\theta > 0$ based on 150, 300, 500 and 1200 training samples respectively.

It can be seen from these results that as the sample size (t) increases, the estimated classes are gradually converging to the original pattern class. ♣

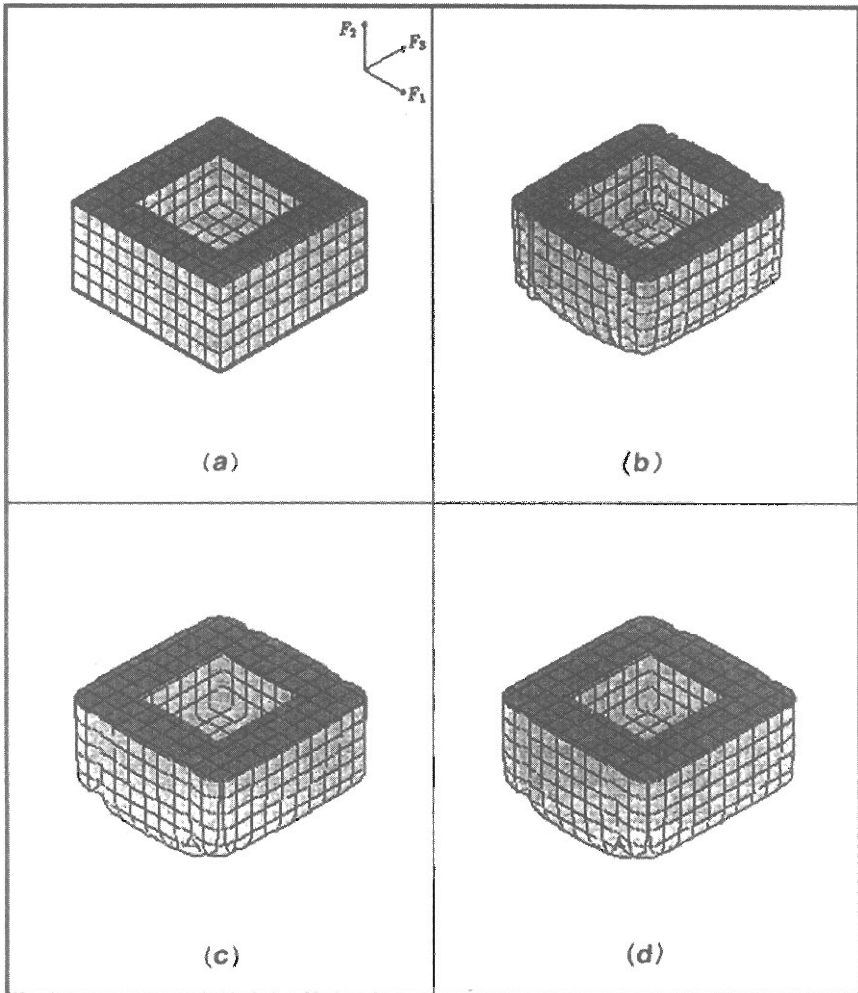


FIGURE 7 (a) Lower segmented portion of a pattern class; (b)–(d) corresponding estimated versions with $\theta \geq 0.5$, $\theta \geq 0.25$, $\theta > 0$ respectively.

B. Criteria for Goodness of Fit

The aforementioned convergence property is also verified analytically using two distance measures (metrics). One of them is the Hausdorff metric and the other one is a similarity metric (*Sim*) defined in Mandal *et al.* [1992a]. It has been shown that the values of both the metrics decrease with the increase in sample size (t).

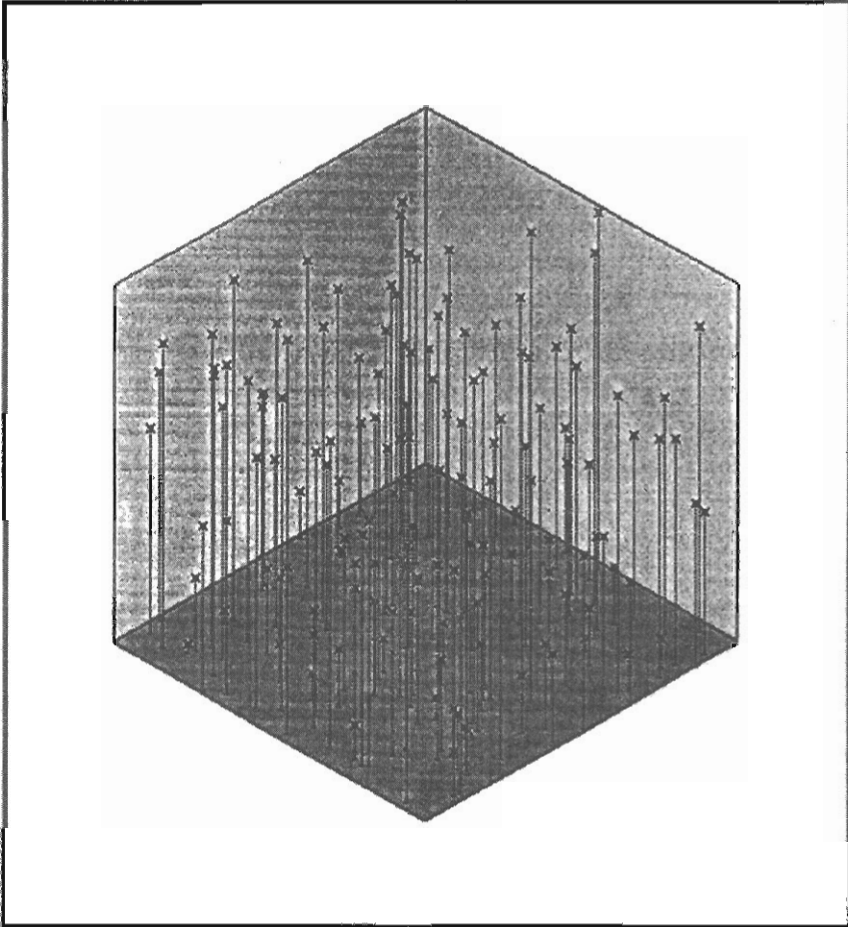


FIGURE 8 A set of training samples from the class in Fig. 5(a).

a. Hausdorff metric: Normally, to find the similarity between sets, a distance measure is often used. Hausdorff metric [Kuratowski 1966] has been used here for this purpose.

Let (X, d) be a metric space. For any compact subset of \mathcal{A} of X , define

$$\delta(y, \mathcal{A}) = \inf_{x \in \mathcal{A}} d(x, y)$$

where inf means infimum. Note that $\delta(y, \mathcal{A})$ is finite and $\exists x_0 \in \mathcal{A}$ such that $\delta(y, \mathcal{A}) = d(x_0, y)$. Now the definition of the Hausdorff metric is given below.

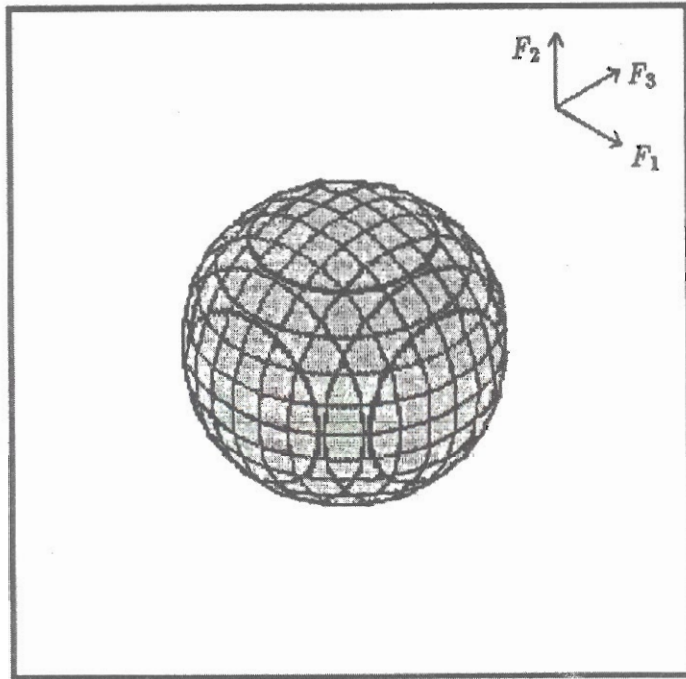


FIGURE 9 A spherical class.

DEFINITION 3 [Kuratowski 1966]: Let \mathcal{A} and \mathcal{B} be two finite compact subsets in \mathbb{R}^N . Then the distance between \mathcal{A} and \mathcal{B} , denoted by $\text{Dist}(\mathcal{A}, \mathcal{B})$, is defined as

$$\text{Dist}(\mathcal{A}, \mathcal{B}) = \max \left\{ \max_{x \in \mathcal{A}} \delta(x, \mathcal{B}), \max_{y \in \mathcal{B}} \delta(y, \mathcal{A}) \right\} \quad (8)$$

where

$$\delta(x, \mathcal{B}) = \min_{y \in \mathcal{B}} d(x, y)$$

and

$$\delta(y, \mathcal{A}) = \min_{x \in \mathcal{A}} d(x, y).$$

This distance measure $\text{Dist}(\mathcal{A}, \mathcal{B})$ is considered here as one of the criteria for goodness of fit, where \mathcal{A} is considered as the boundary of the estimated set or class and \mathcal{B} is considered as the boundary of the original class. This distance measure Dist has also been applied on the estimated sets or classes [figures 10(a)–(d), 11(a)–(d) and 12(a)–(d)] with the original set in Fig. 9. The boundary of the sphere is approximated by 5675 equally spaced points and this set of 5675 points is considered here as the set \mathcal{B} . Three levels of estimated boundary based on the

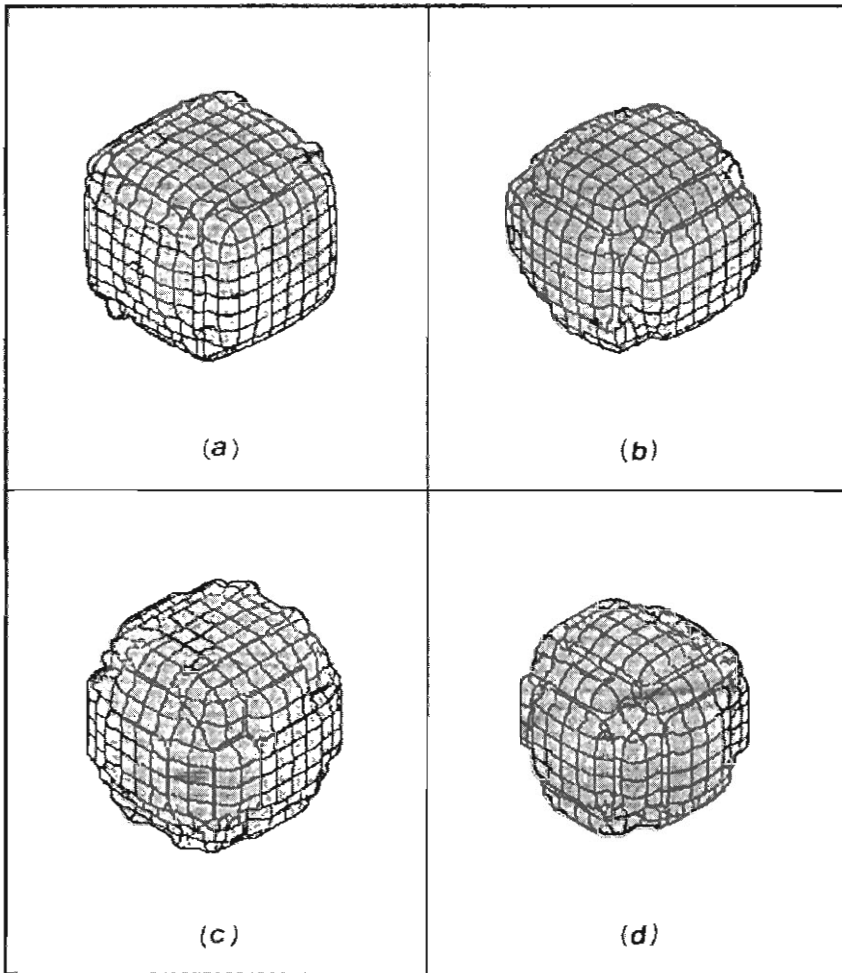


FIGURE 10 (a)–(d) Estimated versions of the class in Fig. 9 with $\theta \geq 0.5$ based on 150, 300, 500 and 1200 samples respectively.

possibility values (θ), namely $\theta \geq 0.5$, $\theta \geq 0.25$ and $\theta > 0$, are considered here. The values of the *Dist* measure are shown by a graph in Fig. 13. ♣

b. Another metric Sim: Note that the Hausdorff metric reflects the overall similarity between two closed sets. In order to incorporate the similarity of each of the elements of the sets, a new measure was defined in Mandal *et al.* [1992a] and it is given below.

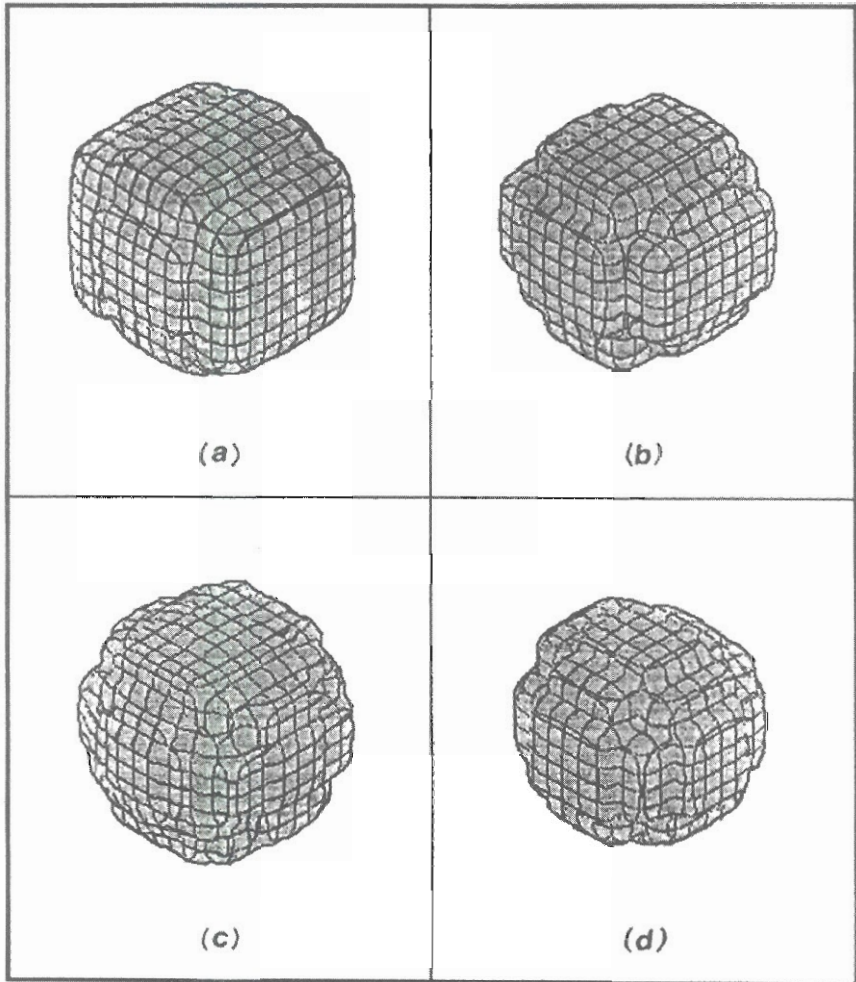


FIGURE 11 (a)–(d) Estimated versions of the class in Fig. 9 with $\theta \geq 0.25$ based on 150, 300, 500 and 1200 samples respectively.

DEFINITION 4: Let \mathcal{A} and \mathcal{B} be two finite subsets in \mathbb{R}^N with $t_{\mathcal{A}}$ and $t_{\mathcal{B}}$ elements respectively. Then a similarity measure between \mathcal{A} and \mathcal{B} , denoted by $\text{Sim}(\mathcal{A}, \mathcal{B})$, is defined as

$$\text{Sim}(\mathcal{A}, \mathcal{B}) = \frac{1}{t_{\mathcal{A}}} \sum_{x \in \mathcal{A}} \delta(x, \mathcal{B}) + \frac{1}{t_{\mathcal{B}}} \sum_{y \in \mathcal{B}} \delta(y, \mathcal{A}) + \text{Dist}(\mathcal{A}, \mathcal{B}) \quad (9)$$

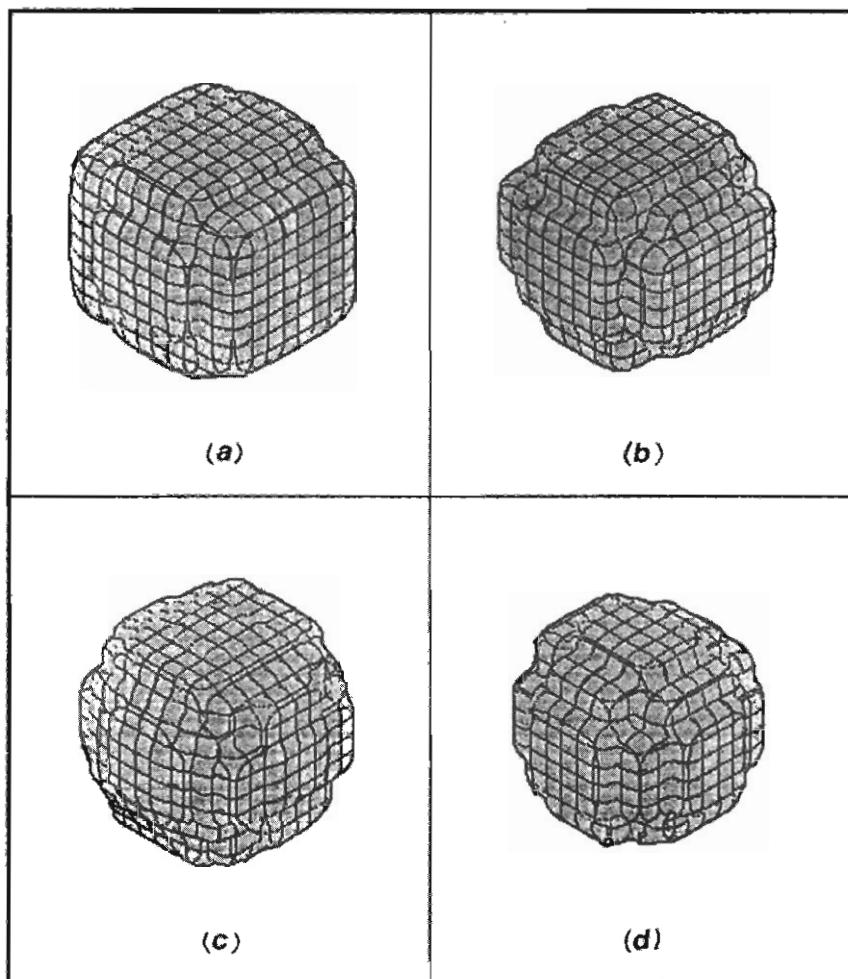


FIGURE 12 (a)–(d) Estimated versions of the class in Fig. 9 with $\theta > 0$ based on 150, 300, 500 and 1200 samples respectively.

Sim is a metric [Mandal *et al.* 1992a; Mandal 1992] and it has been considered here as another criterion for goodness of fit for the shape determining procedure. It has also been applied between the pattern class in Fig. 9 and its estimated multi-valued classes [figures 10(a)–(d), 11(a)–(d) and 12(a)–(d)]. The values of the *Sim* measure are provided in Fig. 14. ♣

Hence, the convergence property of the proposed shape determining procedure is also established for \mathbb{R}^3 . ♠

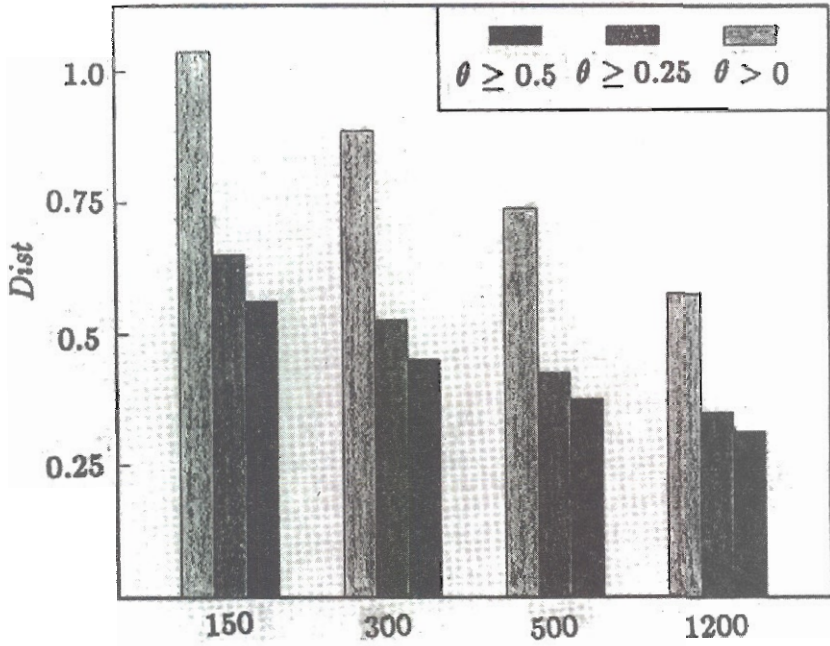


FIGURE 13 Values of *Dist* measure between the actual class in Fig. 9 and its estimated versions

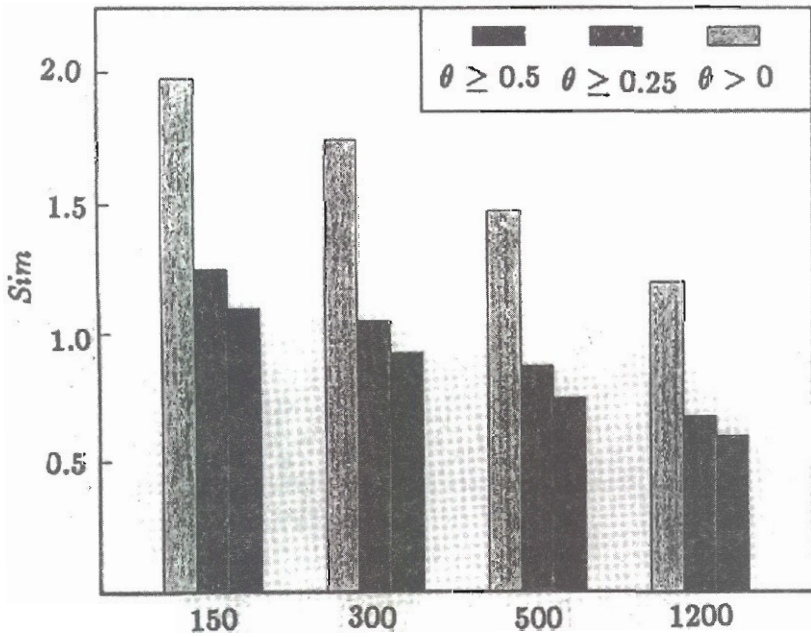


FIGURE 14 Values of *Sim* measure between the actual class in Fig. 9 and its estimated versions.

VIII. CONCLUSIONS AND DISCUSSION

We suggested earlier [Mandal *et al.* 1992a] an approach to compute the multivalued shape of a pattern class from its sampled points in \mathbb{R}^2 . In the present article, an extension of the procedure to higher dimension has been made and the same algorithm is applicable for any value of the dimension (N). (The literature in this context is sparse.) The fuzzy set theory has been found to be an appropriate tool in the solution of this problem. While estimating the shape, the portions not covered by the sampled points are assigned some fuzzy membership values denoting the degrees of their belonging to the actual class. Therefore, unlike the conventional approaches, the proposed method does not attempt to provide crisp boundary from incomplete sample set. The effectiveness of the extended concepts has been demonstrated on some artificially generated data sets in \mathbb{R}^3 . The multivalued shapes can be converted to the usual crisp versions by considering only the feature points (FSC) with possibility value (θ) ≥ 0.5 , say to be within the classes. The convergence of the estimated shape to the original one has been verified both experimentally and analytically.

The parameter to be chosen for the implementation of the proposed method is the *accuracy factor*. According to Grenander [1981], a *good* estimate of the shape can be found if $\delta_t \rightarrow 0$ and $t\delta_t^N \rightarrow \infty$ as $t \rightarrow \infty$. There exist many sequences following these two properties. We have taken one such sequence so that δ_t here satisfies inequality as shown in (1). In fact, we have taken δ_t to be a number close to the average of $\frac{1}{t^N}$ and $\frac{1}{t^{N+1}}$. (Note that $\frac{1}{t^N}$ and/or $\frac{1}{t^{N+1}}$ can be irrationals.) The reason for imposing the above stated conditions on δ_t is elaborately stated in the literature [Grenander 1981].

The *coverage factors* required for determining the shape of a class are determined automatically from δ_t and the sampled points. One of the major underlying features of the procedure is that any pattern class can be represented as a collection of some nearly parallelepiped shaped subclasses. This concept was also found to be very useful in developing a multivalued recognition system [Mandal *et al.* 1992b].

Note that the proposed procedure for finding shapes in \mathbb{R}^N is, seemingly, dependent upon the orientation of the set with respect to feature axes. That is, most of the concepts/blocks regarding our method are based upon the direction of the feature axes. It is apparent that the most likely case for which these blocks may not provide the expected results is the one where the set is situated along the diagonal directions. In such cases, if the axes are rotated by a suitable angle (to make the set lie along the direction of the feature axes), the resultant estimated boundary is likely to be more smooth. This issue was already addressed earlier [Mandal *et al.* 1992a] for the point sets in \mathbb{R}^2 . It may be mentioned that whatever

be the orientation of the original set, the estimated set will tend to it as the number of sampled points goes to ∞ .

The computational complexity of the proposed method increases exponentially with the number of features. Thus complexity needs to be reduced for efficient implementation in higher dimension. Note that our aim has been to develop a generalized approach to determine the shape of a pattern class in any dimension as because the literature in this direction is poor. The problem of reducing the complexity, which has not been addressed here, may constitute a part of future investigation.

References

- Akl, S. K. and G. T. Toussaint (1978) "Efficient convex hull algorithm for pattern recognition applications." In *Proc. 4th Int. St. Conf. on Patt. Recog.*, Kyoto. pp. 483–487.
- Bezdek, J. C. (1981) *Pattern Recognition with Fuzzy Objective Function Algorithms*, Plenum Press, New York.
- Bezdek, J. C. and S. K. Pal (Eds) (1992) *Fuzzy Models for Pattern Recognition*, IEEE Press, New Jersey.
- BOISSONNAT, J. D. (1984) "Geometric structures for three-dimensional shape representation." *ACM Trans. on Graphics*, vol. 3, pp. 266–286.
- Edelsbrunner, H., D. G. Kirkpatrick and R. Seidel (1983) "On the shape of a set of points in a plane." *IEEE Trans. on Inform. Theory*, vol. IT-29, pp. 551–559.
- Edelsbrunner, H. and E. P. Mücke (1992) "Three-dimensional α shapes." In *Proc. Workshop on Volume Visualization*, pp. 75–82.
- Fairfield, J. (1979) "Contoured shape generation forms that people see in dot patterns." In *Proc. IEEE Conf. on Cybern. and Soc.*, pp. 60–64.
- Grenander, U. (1981) *Abstract Inference*. John Wiley, New York.
- Jarvis, R. A. (1977) "Computing the shape hull of points in the plane." In *Proc. IEEE Comp. Soc. Conf. on Patt. Recog. and Image Process*, pp. 231–241.
- Kandel, A. (1982) *Fuzzy Techniques in Pattern Recognition*. Wiley Interscience, New York.
- Kuratowski, K. (1966) *Topology*, vol. I, Academic Press, New York.
- Mandal, D. P., C. A. Murthy and S. K. Pal (1992a) "Determining the shape of a pattern class from sampled points in IR^2 ." *Int. J. of General Systems*, vol. 20, pp. 307–339.
- Mandal, D. P., C. A. Murthy and S. K. Pal. (1992b) "Formulation of a multivalued recognition system." *IEEE Trans. on System, Man & Cyberns.*, vol. SMC-22, pp. 607–620.
- Mandal, D. P. (1992) *A Multivalued Approach for Uncertainty Management in Pattern Recognition Problems Using Fuzzy Sets*. Ph.D. thesis, Indian Statistical Institute, Calcutta, India.
- Murthy, C. A. (1988) *On Consistent Estimation of Classes in IR^2 in the Context of Cluster Analysis*. Ph.D. thesis, Indian Statistical Institute, Calcutta, India.
- Pal, S. K. and D. Dutta Majumder (1986) *Fuzzy Mathematical Approach to Pattern Recognition*. John Wiley (Halsted Press), New York.
- Preparata, F. P. and M. I. Shamos (1985) *Computational Geometry: An Introduction*. Springer Verlag, New York.
- Toussaint, G. T. (1980) "Pattern recognition and geometrical complexity." In *Proc. 5th Int. Conf. on Patt. Recog.*, Miami Beach, Florida, pp. 1324–1347.
- Yager, R. R. and L. A. Zadeh (Eds) (1992) *An Introduction to Fuzzy Logic Applications in Intelligence Systems*. Kluwer Academic Publishers, Boston.
- Zadeh, L. A. (1965) "Fuzzy sets." *Information & Control*, vol. 8, no. 3, pp. 338–353.
- Zadeh, L. A. (1973) "An outline of a new approach to the analysis of complex systems and decision processes." *IEEE Trans. System, Man & Cyberns.*, vol. SMC-3, pp. 28–44.